NOTICE CONCERNING COPYRIGHT RESTRICTIONS

Liquid Holdup in Geothermal Wells

Sabodh K. Garg, John W. Pritchett and James H. Alexander

Science Applications International Corporation (SAIC)
10260 Campus Point Drive, San Diego, CA 92121, USA

Keywords

Holdup correlation, pressure and temperature profiles, well simulators, simulation, two-phase flow, spinner

ABSTRACT

Simulation of two-phase flow in geothermal wellbores requires use of empirical correlations for liquid holdup and for friction factor. Use of currently available correlations often yields widely differing results for geothermal wells. A new liquid holdup correlation is devised for cased wellbores using high-quality discharge and downhole pressure and temperature data from flowing geothermal wells. The latter dataset encompasses a wide range of wellbore diameters, discharge rates and flowing enthalpies. The measured wellhead pressures for wells in the dataset display excellent agreement with the pressures computed by using the new holdup correlation.

Introduction

An ability to predict both the quantity of fluid that can be produced and its thermodynamic state (pressure, temperature, enthalpy, gas content, salinity, *etc.*) is essential for estimating the total usable energy of a geothermal resource. Numerical reservoir simulators can be utilized to calculate the thermodynamic state of the fluid at the underground feed-zone(s) at which the fluid enters the wellbore. The computation of the well-head fluid properties from a given underground state (or vice-versa) requires the use of a wellbore simulator.

Treatment of two-phase flow in a wellbore requires use of empirical correlations for liquid hold-up and friction factor. Because of slip between the gas and liquid phases, the flowing gas quality Q_f is generally different from the *in situ* gas quality Q_s. The liquid hold-up correlation provides a relationship between Q_f and Q_s. Almost all of the existing holdup correlations (see *e.g.* Ansari *et al.*, 1994; Aziz *et al.*, 1972; Beggs and Brill, 1973; Duns and Ros, 1963; Hadgu, 1989; Hagedorn and Brown, 1965; Hughmark, 1962; Hughmark and Pressburg, 1961; Orkiszewski, 1967) are based on flow in two-phase petroleum (oil and gas) systems. At present, there does not exist a sufficient basis for selecting one or another of these correlations to simulate two-phase flow in geothermal wellbores. Utilization of different correlations very often yields widely differing results (see *e.g.* Finger, *et al.*, 1999).

In this paper, we describe the development of new hold-up correlations for geothermal applications using data from flowing geothermal wells. To support this research work, proprietary downhole logs and other required data were supplied by Unocal, Caithness, and various Japanese developers. As a result of a detailed examination of these well data, we identified over 30 wells with high quality discharge (mass discharge rate and enthalpy) and downhole pressure and temperature data. The data set encompasses a wide range of discharge enthalpies (*i.e.* moderate enthalpy wells producing from liquid feedzones, and wells with enthalpies approaching the enthalpy of saturated steam), and casing diameters (ID's ranging from 100 mm to 384 mm). As far as fluid composition is concerned, the data set leaves something to be desired. The salinity and non-condensable gas content of most of the wells in the data set are less than 1.5% and 1% (mass fraction of the produced fluid), respectively. In any event, this data set is eminently suitable for developing a new empirical liquid hold-up correlation for geothermal wells.

Our methodology for developing a hold-up correlation is outlined in Section 2. The downhole pressure/temperature profiles were simulated using an existing wellbore code with an adjustable hold-up correlation. The results of these simulations were employed to generate a multi-parameter data set. The latter data are used in Sections 3 and 4 to relate flowing gas quality to other parameters. Spinner data are employed in Section 5 to provide an independent check on the holdup correlations developed in Sections 3 and 4.

Fluid Flow in Geothermal Wells

The pressure drop associated with two-phase fluid transport in a geothermal well represents the combined effects of friction, acceleration, and the loss of elevation. While the pressure drop

due to acceleration is usually small in single-phase liquid flow in a pipe, it is very often the most important component in two-phase flow. The fluid flow in a geothermal well is not amenable to strict analytical treatment. For two-phase flow, it is necessary to supplement mass, momentum and energy balance relations by empirical correlations for (1) friction factor, and (2) liquid hold-up. In the following, a wellbore simulator, incorporating an existing friction factor correlation and an adjustable liquid hold-up correlation, is used to match the downhole pressure profiles in flowing wells. The simulation results are employed to generate a multi-parameter (flowing quality, static quality, *in situ* liquid and gas volume fractions, gas and liquid viscosities, *etc.*) data set. The latter data sets forms the basis for the development of a new liquid hold-up correlation.

The downhole pressure (and temperature) profiles in the cased portion of flowing wells have been simulated using a specially modified version (see below) of the wellbore computer simulation program WELBOR (Pritchett, 1985). The WELBOR code treats the steady flow of liquid water and steam up a borehole. The user provides parameters describing the well geometry (inside diameter and angle of deviation with respect to the vertical along the hole length), a stable formation temperature distribution with depth, and an "effective thermal conductivity" as a function of depth representing the effects of conductive heat transfer between the fluid in the wellbore and the surrounding formation. For boreholes with two-phase flow at the bottom of the cased portion, the fluid state is prescribed by specifying flowing pressure, flowing enthalpy, salinity, and gas content.

In two-phase water/steam flow, pressure and temperature are not independent of each other. For any reasonable value of effective thermal conductivity κ, the downhole flowing enthalpy may be adjusted to yield the appropriate pressure, and hence temperature, distribution in the wellbore, and flowing wellhead enthalpy. Matching the pressure/temperature distribution in the wellbore and flowing wellhead enthalpy does not constrain the heat loss and downhole enthalpy. Since the flowing downhole enthalpy is not a measured quantity, it is not possible to determine a unique value for heat loss in the presence of two-phase flow. It is, therefore, appropriate to eliminate effective thermal conductivity as a free parameter; for all of the calculations reported hereunder, κ was set equal to 4 W/m-°C).

For the present study, the frictional pressure gradient is computed using the Dukler I correlation (Dukler *et al.*, 1964), and a user prescribed roughness factor, ε. The roughness factor, ε, may vary with depth. For most of the pressure profiles considered herein, the roughness factor was assumed to be zero. In a few cases, it was found necessary to use a non-zero value for ε.

The relative slip between the liquid and gas phases is treated in WELBOR using a modified version of the Hughmark liquid holdup correlation (Hughmark, 1962). The slippage rate may vary between the value given by the Hughmark correlation and no slip at all, according to the value of a user specified parameter, η, which varies between zero (no slip) and unity (Hughmark). For the present application, the WELBOR code was modified so as to allow η to vary as a function of depth. For all of the pressure profiles considered herein, it was found that at most two values of η (and a small transition zone in between) were required to produce a satisfactory match between the measured and computed pressures.

Given the fluid state at the bottom of the cased interval and the mass discharge rate, a wellbore simulator such as WELBOR can be used to compute the fluid state along the wellbore and at the wellhead. The principal parameters that may be varied to match the measured conditions along the wellbore (pressure and temperature) and at the wellhead (pressure, temperature, steam and liquid flow rates, liquid salinity, gas content of steam) are (1) flowing enthalpy, salinity and gas content at the bottom of the cased interval, (2) holdup parameter, η, and (3) interior roughness factor, ε.

To illustrate the computational procedure, it is useful to consider Unocal well A-4 (Garg and Pritchett, 2001). Well A-4 is cased and cemented to a depth of 888.5 mTVD (901.6 mMD). The following well geometry is assumed for the cased section of well A-4:

Measured Depth (meters)	Vertical Depth (meters)	Angle with Vertical (Degrees)	Internal Diameter (mm)
277.4	277.4	0.000	384
901.6	888.5	11.759	315

The measured pressures in the flowing well are in good agreement with the saturation pressure for pure water corresponding to the measured temperatures (Garg and Pritchett, 2001). A pressure of ~23.49 bars (taken as the average of measured and saturation pressures) was recorded in the flowing well at 888.5 mTVD. The reported discharge rate and wellhead enthalpy were 135 kg/s and 1089 kJ/kg, respectively. Total dissolved solids content of the separated liquid was 14600 ppm; the non-condensable gas content of the steam was 0.68%.

The stable formation temperature (Garg and Pritchett, 2001) was approximated by the following temperature distribution using linear interpolations between tabulated data.

Vertical Depth (meters)	Temperature (Degrees Celsius)
0	27
305	68
754	212
888.5	227

The best match to the downhole pressure profile and wellhead fluid state (pressure, enthalpy, salinity, gas content) was obtained using the following values for unknown model parameters:

Flowing enthalpy at 888.5 mTVD = 1102 kJ/kg
Fluid (liquid + steam) salinity
at 888.5 mTVD = 0.012 kg/kg
Fluid (liquid + steam) gas
content at 888.5 mTVD = 0.0011 kg/kg
Hughmark parameter, η = 0.09 for depths < 350 m
= 0.09 + 0.0062 (depth – 350)
for 350 m <depth <400 m
= 0.40 for depths > 400 m
Roughness factor, ε = 0.00 mm for all depths

The computed pressure profile is compared with the measurements in Figure 1; the agreement is excellent. The computed fluid state at the wellhead (fluid enthalpy: 1089 kJ/kg, liquid phase salinity: 14,300 ppm; steam phase gas content: 0.67%) is very close to the measurements.

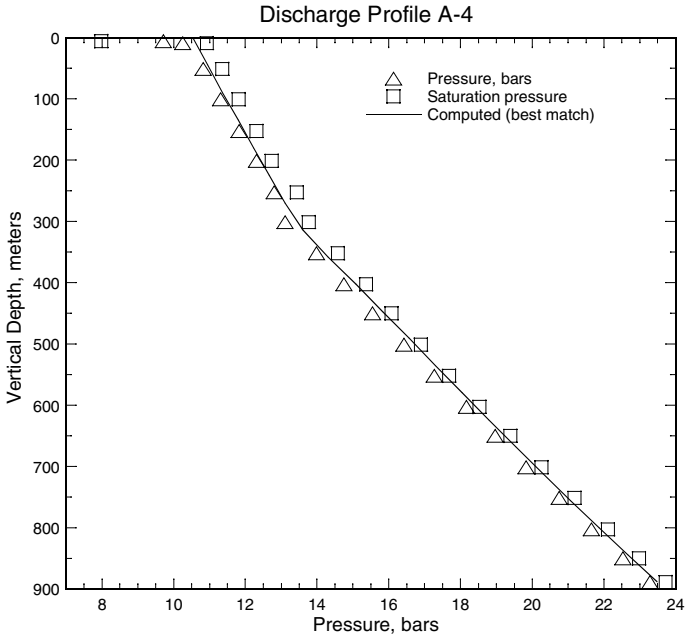

Figure 1. Pressure profile (triangle) recorded in discharging well A-4. The squares indicate saturation pressure corresponding to local measured temperature. The solid line is the computed pressure profile.

An essentially identical procedure was used to fit the downhole pressure and wellhead fluid state measurements for all of the wells in the dataset (see Garg *et al.*, 2004 for details). The data for the Unocal wells (and presumably the single Caithness well) were obtained while these wells were discharging in a more or less stable manner. Available data for these wells include the NCG and salt content of the discharge stream. By way of contrast, data for the Japanese wells were obtained during short term discharge tests. No NCG and salinity measurements are available for the production fluid from these short term tests. Also, discharge rate and wellhead enthalpy measurements from the short term tests may not be very accurate; these errors are likely to be most problematical for wells with very low discharge rates. Although flow data for the Japanese wells in the dataset are liable to be less accurate than for the Unocal wells, it was decided against discarding these data in that the Japanese well test data are typical of relatively high quality measurements taken during the exploration phase.

The results of these downhole pressure/temperature simulations (Garg *et al.*, 2004) were used to define the fluid state and associated quantities (*e.g.* liquid and gas velocities) in the cased section of all the wells in the dataset. Somewhat arbitrarily, it was decided to use 21 equally spaced points along each downhole profile to create a dataset (see Table 2.1 in Garg *et al.*, 2004 for an example) for formulating a new holdup correlation.

A New Holdup Correlation

Duns and Ros (1963) suggest that the various flow regimes that accompany two-phase flow in wells can be divided into three main regions depending on the gas throughput (Figure 2). The axes in Figure 2 denote the non-dimensional liquid and gas velocity numbers:

Liquid velocity number, $N_l = S_l v_l (\rho_l / g\sigma)^{0.25}$

Gas velocity number, $N_g = S_g v_g (\rho_g / g\sigma)^{0.25}$

Here $\nu_l (\nu_g)$ is the liquid (gas) velocity, $S_l (S_g)$ is the *in situ* liquid (gas) volume fraction, $\rho_l (\rho_g)$ is the liquid (gas) density, g is the acceleration due to gravity, and σ is the surface tension. Region I has a continuous liquid phase, and contains bubble flow, plug flow and part of froth-flow regimes. Liquid and gas phases alternate in Region II covering the slug flow and remainder of the froth-flow regimes. Region III is characterized by a continuous gas phase, and contains the mist-flow regime.

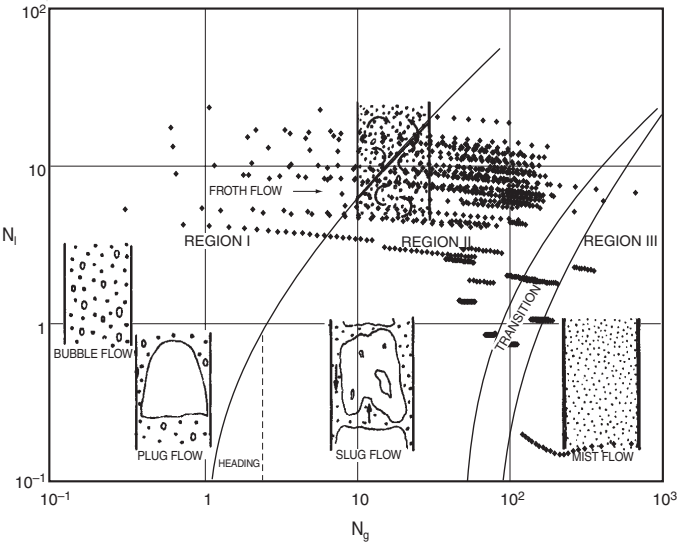

Figure 2. Two-phase fluid flow regimes according to Duns and Ros (1963). Also shown (as diamonds) are the data from geothermal boreholes (see Section 2 above).

Data from two-phase geothermal wells are shown as diamonds in Figure 2. Although the geothermal data lie in all the three regions, the bulk of these data are contained in Region II. It appears from Figure 2 that relatively high liquid velocities characterize geothermal wells such that only froth-flow (Regions I and II) and mist-flow (Region III) are encountered in geothermal wells. Once the geothermal fluid starts flashing in the wellbore, the gas (and hence liquid) velocity increases rapidly. Thus, bubble flow, plug flow and slug flow regimes, if present at all, are likely to be confined to a narrow depth range and difficult to observe. Because of the limited range of flow regimes, it should be possible to describe two-phase flow in geothermal wells by a single (or at most a two-part) holdup correlation.

The flowing quality Q_f (=gas flow rate/total flow rate) is defined as follows:

$$Q_f = \frac{AS_g\rho_g v_g}{M} \tag{1}$$

where A is the internal cross-sectional area of the pipe, and M is the total mass flow rate. Bankoff (1960) derived a relation for flowing quality Q_f that is equivalent to:

$$Q_f = \frac{Q_s}{[1-Q_s]K + Q_s\left[1-\rho_l(1-K)/\rho_g\right]} \tag{2}$$

where Q_s *is* the *in situ* (or static) quality, ρ_m is the mixture (gas plus liquid) density, and K is a flow parameter (see below).

$$Q_s = \frac{S_g\rho_g}{\rho_m} \tag{3}$$

$$\rho_m = S_l\rho_l + S_g\rho_g \tag{4}$$

For the case of homogeneous (*i.e.* no slip) flow, the *in situ* quality Q_s is equal to the flowing quality Q_f; furthermore, flow parameter K is identically equal to unity. In general, one would expect the gas phase to rise more rapidly in the well than the liquid phase due to buoyancy; this implies that

$$Q_f \geq Q_s \tag{5a}$$

$$S_g \leq K \leq 1 \tag{5b}$$

The two-phase flow in a well is influenced by buoyancy, inertial, viscous and surface tension forces (Bankoff, 1960). Based on dimensional arguments, Hughmark (1962) concluded that the flow parameter K might be expected to depend on the flowing liquid volume fraction Y_l, and Reynolds (Rn), Froude (Fr), and Weber (We) numbers.

$$Y_l = \frac{S_l v_l}{(S_l v_l + S_g v_g)}$$

$$Rn = \frac{d_w M}{A\mu_m} \tag{6a-d}$$

$$Fr = \frac{M^2}{(d_w A^2 g\rho_m^2)}$$

$$We = \frac{d_w^2 g\rho_g Fr}{\sigma}$$

Here d_w is the inside well diameter, σ is the liquid surface tension, and μ_m is the mixture viscosity.

$$\mu_m = S_l\mu_l + S_g\mu_g \tag{7}$$

In Equation (7), μ_l (μ_g) denotes the liquid (gas) viscosity.

Mixture (liquid plus gas) density ρ_m and mixture viscosity μ_m can be defined in a number of ways (see *e.g.* Hughmark, 1962; Dukler, *et al.*, 1964); in the following, the expressions given by Hughmark, Equations (4) and (7), will be used. The latter definitions for ρ_m and μ_m are different than those used by Dukler, *et al.* (1964).

To find a correlation for K, it is assumed that K can be expressed as a function of a single variable Z:

$$K = K(Z(Rn, Fr, Y_l, We, S_l)) \tag{8}$$

Hughmark (1962) investigated the dependence of Z on Rn, Fr, Y_l, and We, and found that Z (and hence K) did not appreciably depend on the Weber number (We). The authors have independently confirmed the latter result using data for geothermal wells (Section 2). Consequently, Z is assumed to depend on only four variable, *i.e.*, Rn, Fr, Y_l and S_l; note that Hughmark (1962) did not account for the dependence of Z on S_l. Following Hughmark (1962), we introduce a particularly simple relationship for Z:

$$Z = Rn^{\alpha} Fr^{\beta} Y_l^{\gamma} S_l^{\omega} \tag{9}$$

where α, β, γ, and ω are as yet undetermined constants. Determination of the exponents in Equation (9) is straightforward when the functional relationship between K and Z is known; in this case, exponents can be estimated by minimizing the variance between the calculated (*i.e.* from the functional relationship K-Z) and measured (*i.e.* those derived from fitting the flow data in Section 2) values for K. Unfortunately, the functional relationship $K(Z)$ is unknown, and must be determined from the dataset.

To determine the exponents in Equation (9), we introduce a nonparametric measure of variation. Given a candidate set of exponents, we calculate Z for each point in the dataset for geothermal wells (Section 2, and Figure 2). Next, we sort the dataset in order of increasing Z, and calculate a pseudo-variance *S.V.* as follows:

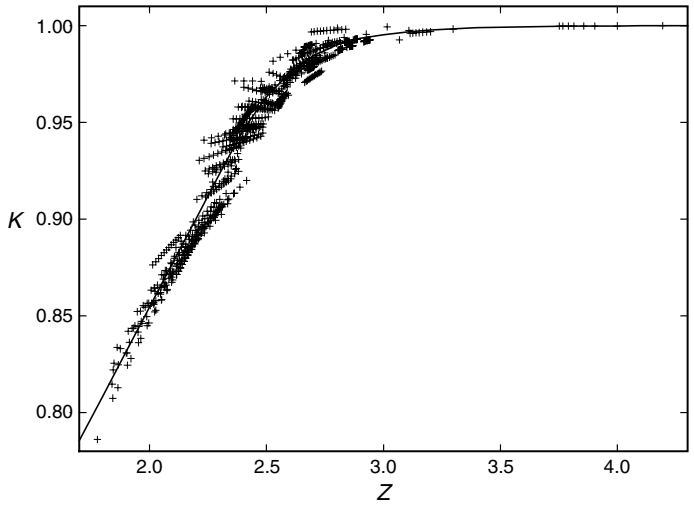

Figure 3. A plot of K versus Z. Data points (+), *i.e.* K versus Z values, in the figure were obtained by minimizing the pseudo-variance. Z is defined by Equation (9) with α = 0.0388887, β = 0.0065170, γ = –0.0002960, and ω = –0.1.The solid line denotes an analytical fit to the K-Z data.

$$S.V. = \sum_{i=1}^{n-1} (K_{i+1} - K_i)^2 \quad (10)$$

Here K_i denotes the value of K corresponding to Z_i, n is the number of points in the dataset, and Z_n is the largest value of Z. The exponents in Equation (9) are obtained by minimizing this pseudo-variance.

The function $K(Z)$ looks like a hyperbola with $K = 1$ as an asymptote (see *e.g.* Figure 3). Although a hyperbola for $K(Z)$ can be made to yield a pseudo-variance that is close to the minimum, a more general functional form for $K(Z)$ is needed in order to improve the fit in regions of Z that make little contribution to the pseudo-variance.

To verify that the holdup correlation (*i.e.* $K(Z)$ relationship) developed herein can be used to simulate two-phase flow in geothermal wells, a special version of WELBOR code was created; this version was configured to use the $K(Z)$ relation (solid line) shown in Figure 3. The latter version of WELBOR was employed to simulate flow data for all the wells in the dataset. Except for the holdup correlation, these simulations utilized the parameters used in the calculations described in Section 2.

Table 1. Comparison of wellhead pressures for high mass velocity profiles (mass velocity > 687 kg/s-m^2) computed using the correlation for $K(Z)$ with data.

Well	*P*-data	*P*-comp	δP***
A-1	8.94	9.51	–0.57
A-2	8.78	9.22	–0.44
A-4	10.53	10.75	–0.22
A-6	14.70	15.15	–0.45
A-7	12.85	11.23	1.62
A-8	9.75	9.66	0.09
A-9	14.56	14.17	0.39
A-10	11.39	10.59	0.80
A-11	11.16	11.79	–0.63
A-12	12.14	12.12	0.02
A-13	12.18	11.79	0.39
A-14	10.98	10.86	0.12
A-16	10.36	10.89	–0.53
A-19	9.61	9.59	0.02
A-20	10.12	10.26	–0.14
A-21	10.52	9.77	0.75
B-5	10.97	10.26	0.71
C-6	9.55	7.68	1.87
KE1-4a	4.26	Choke @ 3.7m*	NA
KE1-4b	3.98	Choke @ 88.9m	NA
KE1-17a	6.64	7.11	–0.47
KE1-19Sa	3.53	Choke @7.6m**	NA
KE1-19Sb	6.37	6.61	–0.24
KE1-22b	7.37	8.15	–0.78
GH-11a	12.23	12.12	0.11
GH-11b	10.51	10.10	0.41
GH-20a	14.14	14.56	–0.42
GH-20b	13.02	13.59	–0.57
GH-20c	11.70	12.43	–0.73
		Total (26 profiles)	1.11

* At 6.9 kg/s, p = 2.31 bars; 6.8 kg/s, p = 2.66 bars; 6.5 kg/s, p = 3.28 bars
** At 23.0 kg/s, p = 3.66 bars.
*** $\delta P = P$-data – P-comp

The computed results for wellhead pressure for all the high mass velocity (mass velocity = total discharge rate / pipe cross-sectional area > 687 kg/s-m^2. The low mass velocity profiles are considered separately in Section 4.) profiles are compared with data (*i.e.* wellhead pressures computed by matching downhole pressure profiles in Section 2) in Table 1. The $K(Z)$ fit yields satisfactory agreement between data and computed wellhead pressures (Table 1); the root-mean-square error is only 0.67 bars.

It is apparent from Table 1 that the above-derived correlation for $K(Z)$ leads to choking for three pressure profiles (KE1-4a, KE1-4b, KE1-19Sa). Well KE1-4 is a slim hole (internal diameter = 10.2 cm), and the downhole profiles were recorded during a short-term discharge test. The reported discharge rates for KE1-4 may be in substantial error. The computed maximum discharge rate for KE1-4 is around 6.9 kg/s, which is within the likely error band for the reported discharge rate for KE1-4. For KE1-19Sa, the computed value for the maximum discharge rate (23.0 kg/s) is within 4% of the nominal discharge rate (23.9 kg/s). Thus, it can be concluded that the $K(Z)$ fit gives acceptable results for these three profiles as well.

As mentioned above, downhole pressure profiles for all the high mass velocity cases in the dataset (Table 1) were simulated using the correlation for $K(Z)$. In most cases, the latter computed profiles are in good agreement with (1) measurements, and (2) calculated profile (best-match) using an adjustable holdup correlation (Section 2). A typical example (well A-4) is shown in Figure 4; the computed pressure profile for well A-4, shown as a dashed line in Figure 4, is in excellent agreement with the measurements.

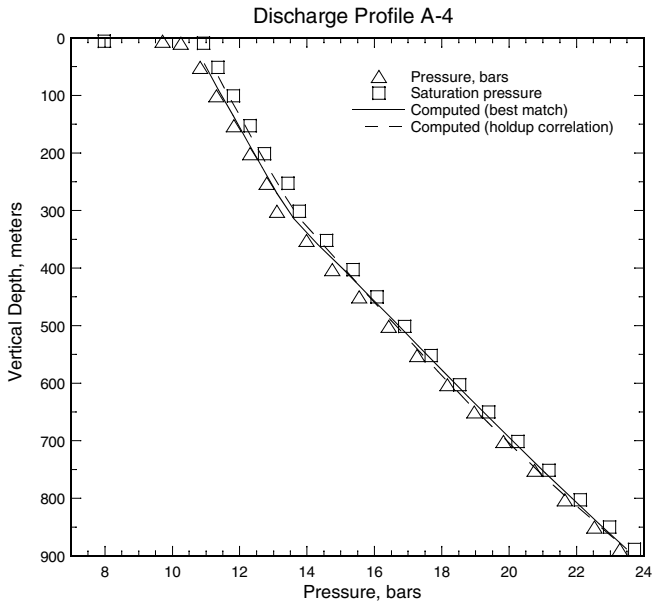

Figure 4. Pressure profile (triangles) recorded in discharging well A-4. The squares indicate saturation pressure corresponding to the local measured temperature. The solid line is the computed pressure profile using an adjustable holdup correlation (see Section 2 for details). The computed pressure profile using the correlation for $K(Z)$ is shown as a dashed line.

Holdup Correlation for Low Mass Velocity

The correlation for $K(Z)$ developed in the preceding section was found to yield satisfactory results for all the high mass velocity (mass velocity > 687 kg/s-m^2) profiles in the dataset. The computed pressures for low mass velocity (mass velocity < 650 kg/s-m^2) profiles are, however, too high, and imply that the correlation for $K(Z)$ would need to be modified for low mass velocity. Attempts to develop a single correlation for both the high and low mass velocity cases by including an additional variable (*i.e.* mass velocity) in the relation for Z (Equation 9) were unsuccessful. Accordingly, it was decided to consider the low mass velocity profiles separately. The $K(Z)$ correlation for the latter case is shown in Figure 5.

The computed results for wellhead pressure for all the low mass velocity (mass velocity = total discharge rate / pipe cross-sectional area < 650 kg/s-m^2.) profiles are compared with data (*i.e.* wellhead pressures computed by matching downhole

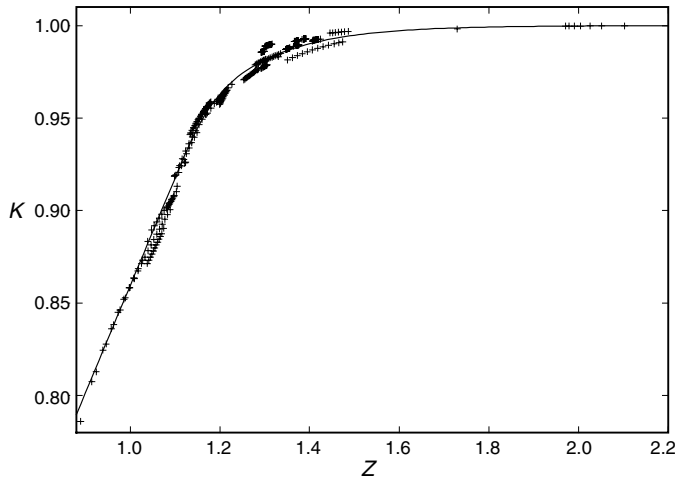

Figure 5. A plot of K versus Z for low mass velocity (mass velocity < 650 kg/s-m^2) profiles. Data points (+), *i.e.* K versus Z values, in the figure were obtained by minimizing the pseudo-variance. Z is defined by Equation (9) with α = –0.009546812, β = 0.00975959, γ = –0.000149868, and ω = –0.1. The solid line denotes an analytical fit to the K-Z data.

pressure profiles in Section 2) in Table 2. The $K(Z)$ fit shown in Figure 5 yields satisfactory agreement between data and computed wellhead pressures (Table 2); the root-mean-square error is 0.73 bars.

As for the high mass velocity cases, the downhole pressure profiles for all the low mass velocity cases in the dataset (Table 2) were simulated using the correlation for K (solid line, Figure 5). The latter computed profiles are for the most part in good agreement with (1) measurements, and (2) calculated profile (best-match) using an adjustable holdup correlation (Section 2).

Comparison with Spinner Data

The rotational speed of a spinner is proportional to the mass-averaged velocity of the fluid mixture passing through the spinner. Except for annular flow, the mass-averaged velocity indicated by the spinner should correspond closely to the mass-averaged velocity of the entire flow stream (Gang, *et al.*, 1990). The spinner response f is related to mass-averaged fluid velocity ν_m and cable speed ν_c as follows:

$$f = m(v_m - v_c) + c \tag{11}$$

where m and c are the calibration constants.

The mass-averaged mixture velocity ν_m can be computed from the *in situ* liquid and vapor saturations, densities, and velocities.

$$v_m = \frac{(\rho_l S_l v_l + \rho_g S_g v_g)}{(\rho_l S_l + \rho_g S_g)} \tag{12}$$

In geothermal wells, the liquid (*i.e.* water) density is much greater than the vapor (*i.e.* steam) density; this means that the mass-averaged mixture velocity is a strong function of the *in situ* liquid volume fraction S_l. Thus matching the spinner data can provide an independent check on the holdup correlations developed in Sections 3 and 4.

Comparison of spinner data with the computed fluid velocity requires a certain amount of care. Spinner data are often quite noisy in two-phase flow, and must be smoothed for a meaningful comparison. In addition, spinner surveys often display anomalous response (*e.g.* a decrease or no change in rotation rate as the spinner tool is traversed up the hole, or a less than commensurate change in rotation rate at a discontinuous change in well diameter) due to improper centering of the tool in the well or a possible temporary flow obstruction in the spinner tool. Obviously, such spinner data must be discarded.

The smoothed spinner data for well A-4 are compared with the computed spinner response in Figure 6. The spinner data for well A-4 (Figure 6) exhibit an anomalous response (decrease/no change in the rotation rate) in the depth range 0–150 m. As can be seen from Figure 6, except for the depth

Table 2. Comparison of wellhead pressures for low mass velocity profiles (mass velocity < 650 kg/s-m^2) computed using the correlation for $K(Z)$ shown in Figure 5 with data.

Well	P-data	P-comp	δP^{**}
A-18	8.19	8.99	–0.80
C-1	10.35	10.35	0.00
C-2	11.58	11.69	–0.11
C-3	11.74	10.92	0.82
C-4	12.43	12.15	0.28
C-5	13.88	14.64	–0.76
B-3	16.27	16.70	–0.43
B-4	18.70	17.96	0.74
B-13	11.76	10.57	1.19
KE1-9	8.59	8.74	–0.15
KE1-11	18.66	17.29	1.37
KE1-17b	7.11	7.38	–0.27
KE1-22a	7.82	8.22	–0.40
S-2	1.15	2.50	–1.35
CS-1	3.97	4.06	–0.09
		Total (15 profiles)	0.04

** δP = P-data – P-comp

range 0–150 m, the smoothed spinner response shows a good agreement with the computed curve. Similar results for all the other wells with spinner data are given in Garg, *et al.* (2004). Barring very few exceptions; the spinner measurements are in good agreement with the computed response (Garg, *et al.,* 2004). Thus, taken as a whole, the spinner measurements tend to validate the holdup correlations developed in Sections 3 and 4.

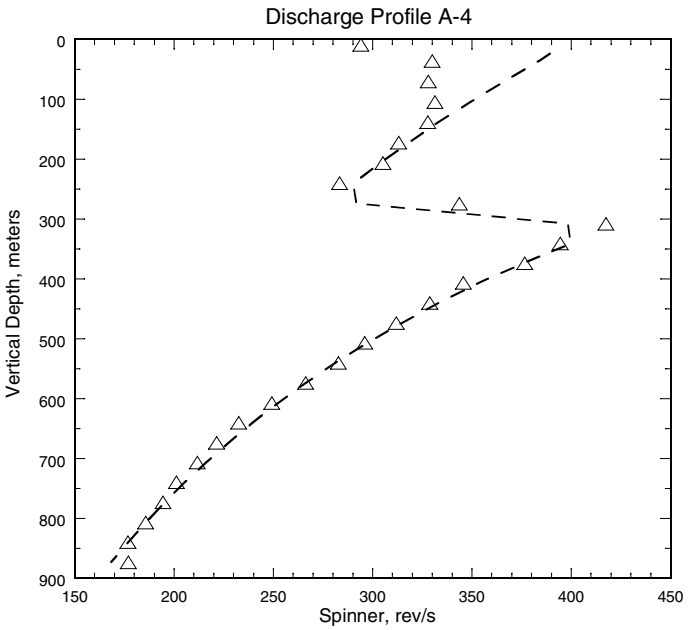

Figure 6. Comparison of the smoothed spinner response (triangles) with the computed spinner response (dashed line) for well A-4.

Concluding Remarks

The principal goal of the present work is to use high quality data from flowing geothermal wells to devise new liquid holdup correlations for geothermal applications. To make the problem tractable, it was decided to at first develop a holdup correlation for only the cased section of geothermal wells. The holdup correlation presented in the preceding sections displays considerable promise for simulating two-phase flow in the cased section of geothermal wells. Future plans call for the formulation of a holdup correlation for the open hole/slotted liner section of geothermal wells.

Acknowledgements

This manuscript has been authored by a contractor of the U.S. government under DOE Contract DE-AC07-99ID13727. Accordingly, the U.S. Government retains a nonexclusive, royalty-free license to publish or reproduce the published form of this contribution, or allow others to do so, for U.S. Government purposes. We also wish to express our thanks to Unocal Corporation and Caithness Operating Company LLC for making their proprietary well data available for this study.

References

Ansari, A. M., N. D. Sylvester, C. Sarica, O. Shoham, and J. P. Brill, 1994. "A Comprehensive Mechanistic Model for Upward Two-Phase Flow in Wellbores." SPE Production & Facilities, p. 143–165, May.

Aziz, K., G. Govier, and M. Fogarasi, 1972. "Pressure Drop in Wells Producing Oil and Gas." Journal Canadian Petroleum Technology, No. 4, p. 38–48.

Bankoff, S. G., 1960. "A variable density single-fluid model for two-phase flow with particular reference to steam-water flow." Journal of Heat Transfer, ASME Transactions, Series C, v. 82, p. 265–272.

Beggs, H. D. and J. P. Brill, 1973. "A Study of Two-Phase Flow in Inclined Pipes." Journal of Petroleum Technology, p. 607–617, May.

Dukler, A. E., M. Wickes III, and R. G. Cleveland, 1964. "Frictional Pressure Drop in Two-Phase Flow: B. An Approach Through Similarity Analysis." A.I.Ch.E. Journal, v. 10(1), p. 44–51.

Duns, H., and N. C. J. Ros, 1963. "Vertical Flow of Gas and Liquid Mixtures in Wells." In: Proceedings 6th World Petroleum Congress, Section II, Paper 22–PD 6, Frankfurt Am Main, Germany, p. 451–465,

Finger, J., R. Jacobsen, C. Hickox, J. Combs, G. Polk, and C. Goranson, 1999. "Slimhole Handbook: Procedures and Recommendations for Slimhole Drilling and Testing in Geothermal Exploration." Report No. SAND99-1976, Sandia National Laboratories, Albuquerque, New Mexico, October.

Gang, X. Z., M. Golan, and J. Sveen, 1990. "Determining Downhole Flow Rates of Oil and Gas in Oil Wells Using Pressure Drop and Spinner Response Measurements." Paper No. 20893, Society of Petroleum Engineers, Dallas, Texas.

Garg, S. K. and J. W. Pritchett, 2001. "Development of New Geothermal Wellbore Holdup Correlations Using Flowing Well Data." Report No. SAIC-01/1061, Science Applications International Corporation, San Diego, California, October.

Garg, S. K., J. W. Pritchett, and J. H. Alexander, 2004. "Development of New Geothermal Wellbore Holdup Correlations Using Flowing Well Data." Report No. SAIC-03/1037**,** Science Applications International Corporation, San Diego, California, March.

Hadgu, T., 1989. "Vertical Two-Phase Flow Studies and Modeling of Flow in Geothermal Wells." Ph.D. Thesis, University of Auckland, Auckland, New Zealand, July.

Hagedorn, A. R. and K. E. Brown, 1965. "Experimental Study of Pressure Gradients Occurring During Continuous Two-Phase Flow in Small-Diameter Vertical Conduits." Journal of Petroleum Technology, p. 475–484, April.

Hughmark, G. A., 1962. "Holdup in gas-liquid flow." Chemical Engineering Progress, v. 53(4), p. 62–65.

Hughmark, G. A., and B. S. Pressburg, 1961. "Holdup and Pressure Drop with Gas-Liquid Flow in a Vertical Pipe." A.I.Ch.E. Journal, v. 7(4), p. 677–682.

Orkiszewski, J., 1967. "Predicting Two-Phase Pressure Drops in Vertical Pipe." Journal of Petroleum Technology, p. 829–838, June.

Pritchett, J. W., 1985. WELBOR: A Computer Program for Calculating Flow in a Producing Geothermal Well. Report No. SSS-R-85-7283, S-Cubed, La Jolla, California (now Science Applications International Corporation, San Diego, California).